Inorg. Chem. **2005**, *44*, 6623–6631

Synthesis of $PtRu_5(CO)_{14}(PBu^t_3)(\mu\text{-}H)_2(\mu_6\text{-}C)$ and Its Reactions with $Pt(PBu^t_3)_2$, $HGePh_3$, and $HSnPh_3$

Richard D. Adams,* Burjor Captain, and Lei Zhu

Department of Chemistry and Biochemistry, University of South Carolina, Columbia, South Carolina 29208

Received June 20, 2005

Reaction of $PtRu_5(CO)_{15}(PBu^t_3)(C)$, **3**, with hydrogen at 97 °C yielded the new dihydride-containing cluster compound $PtRu_5(CO)_{14}(PBu^t_3)(\mu\text{-}H)_2(\mu_6\text{-}C)$, **5**. Compound **5** was characterized crystallographically and was shown to contain an octahedral cluster consisting of one platinum and five ruthenium atoms with a carbido ligand in the center. Two hydrido ligands bridge two oppositely positioned PtRu bonds. Compound **5** reacts with $Pt(PBu^t_3)_2$ to yield $Pt_2Ru_5(CO)_{14}(PBu^t_3)_2(\mu\text{-}H)_2(\mu_6\text{-}C)$, **6**, a $Pt(PBu^t_3)$ adduct of **5**, by adding a $Pt(PBu^t_3)$ group as a bridge across one of the Ru–Ru bonds in the square base of the Ru_5 portion of the cluster. Compound **6** is dynamically active on the NMR time scale by a mechanism that appears to involve a shifting of the $Pt(PBu^t_3)$ group from one Ru–Ru bond to another. Two new complexes, $PtRu_5(CO)_{13}(PBu^t_3)(\mu\text{-}H)_3(GePh_3)(\mu_5\text{-}C)$, **7**, and $PtRu_5(CO)_{13}(PBu^t_3)(\mu\text{-}H)_2(\mu\text{-}GePh_2)(\mu_6\text{-}C)$, **8**, were obtained from the reaction of **5** with $HGePh_3$. The cluster of **7** has an open structure in which the $Pt(PBu^t_3)$ group bridges an edge of the square base of the square pyramidal Ru_5 cluster. Compound **7** also has three bridging hydrido ligands and one terminal $GePh_3$ ligand. When heated to 97 °C, **7** is slowly converted to **8** by cleavage of a phenyl group from the $GePh_3$ ligand and elimination of benzene by its combination with one of the hydrido ligands. The $PtRu_5$ metal cluster of **8** has a closed octahedral shape with a $GePh_2$ ligand bridging one of the Ru–Ru bonds. Two tin-containing compounds, $PtRu_5(CO)_{13}(PBu^t_3)(\mu\text{-}H)_3(SnPh_3)(\mu_5\text{-}C)$, **9**, and $PtRu_5(CO)_{13}(PBu^t_3)(\mu\text{-}H)_2(\mu\text{-}SnPh_2)(\mu_6\text{-}C)$, **10**, which are analogous to **7** and **8** were obtained from the reaction of **5** with $HSnPh_3$.

Introduction

In recent studies, we have shown that the compounds $M(PBu^t_3)_2$, M = Pd or Pt, readily react with metal cluster complexes by adding $M(PBu^t_3)$ groups across one or more metal−metal bonds to form electronically unsaturated higher-nuclearity bimetallic complexes.[1,2] Examples of some of these products include $Ru_3(CO)_{12}[Pd(PBu^t_3)]_3$, **1**,[1a] $Ru_6(CO)_{17}(\mu_6\text{-}C)[Pd(PBu^t_3)]_2$, **2**,[1a] and $PtRu_5(CO)_{15}(PBu^t_3)(C)$, **3**.[2] Interestingly, compound **3** exists in solution as a mixture of two isomers, a closed one, **3a**, and an open one, **3b**, that inter-

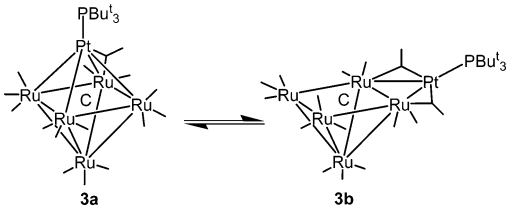

3a **3b**

convert rapidly on the NMR time scale. Compound **3** reacts with PhC_2H to yield the alkyne complex $PtRu_5(CO)_{13}(PBu^t_3)(\mu_3\text{-}PhC_2H)(\mu_5\text{-}C)$, **4**, in which the cluster has an open

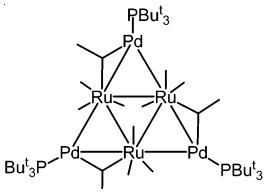

1

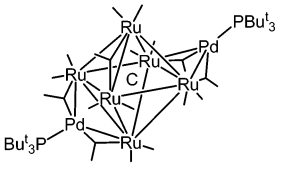

2

* To whom correspondence should be addressed. E-mail: Adams@mail.chem.sc.edu.

(1) (a) Adams, R. D.; Captain, B.; Fu, W.;Hall, M. B.; Manson, J.; Smith M. D.; Webster, C. E. *J. Am.* Chem. Soc. **2004**, *126*, 5253. (b) Adams, R. D.; Captain, B.; Pellechia, P. J.; Zhu, L. *Inorg. Chem.* **2004**, *43*, 7243. (c) Adams, R. D.; Captain, B.; Smith M. D. *J. Cluster Sci.* **2004**, *15*, 139. (d) Adams, R. D.; Captain, B.; Johansson, M.; Smith J. L., Jr. *J. Am. Chem. Soc.* **2005**, *127*, 488.

(2) Adams, R. D.; Captain, B.; Fu, W.; Pellechia, P. J.; Smith, M. D. *Inorg. Chem.* **2003**, *42*, 2094.

10.1021/ic051007q CCC: $30.25
Published on Web 08/18/2005

structure related to that of **3b**, and with H_2 to yield the dihydride complex $PtRu_5(CO)_{14}(PBu^t_3)(\mu\text{-}H)_2(\mu_6\text{-}C)$, **5**, in which the cluster has a closed structure related to that of **3a**.[3]

Bimetallic cluster complexes such as these have recently been shown to be valuable precursors to bimetallic nanoparticle catalysts when placed on mesoporous supports.[4] Here we report the synthesis and characterization of the dihydrido cluster complex $PtRu_5(CO)_{14}(PBu^t_3)(\mu\text{-}H)_2(\mu_6\text{-}C)$, **5**, obtained from the reaction of **3** with hydrogen and the results of our studies of the reactions of **5** with $Pt(PBu^t_3)_2$ and the compounds $HGePh_3$ and $HSnPh_3$.

Experimental Section

General Data. All reactions were performed under a nitrogen atmosphere by using Schlenk techniques. Reagent-grade solvents were dried by the standard procedures and were freshly distilled prior to use. Infrared spectra were recorded on an AVATAR 360 FT-IR spectrophotometer. ^{1}H NMR and ^{31}P{^{1}H} NMR were recorded on a Varian Mercury 400 spectrometer operating at 400 and 162 MHz, respectively. ^{31}P{^{1}H} NMR spectra were externally referenced against 85% *ortho*-H_3PO_4. ^{1}H NMR spectra at various temperatures were recorded on a Varian Innova 500 spectrometer operating at 500 MHz. Elemental analyses were performed by Desert Analytics (Tucson, AZ). $Pt(PBu^t_3)_2$ was purchased from Strem. $HGePh_3$ and $HSnPh_3$ were purchased from Aldrich and were used without further purification. $PtRu_5(CO)_{15}(PBu^t_3)(C)$ was prepared according to the published procedure.[2] Product separations were performed by TLC in air on Analtech 0.25 and 0.5 mm silica gel 60 Å F_{254} glass plates.

Synthesis of $PtRu_5(CO)_{14}(PBu^t_3)(\mu\text{-}H)_2(\mu_6\text{-}C)$, 5. A 9.3 mg amount of **3** (0.0070 mmol) was dissolved in 10 mL of heptane in a 25 mL three-neck flask. The solution was then heated to reflux and purged with hydrogen (1 atm) for 1.5 h. The solvent was then removed in vacuo and the product was separated by TLC by using a 4:1 hexane/methylene chloride solvent mixture to yield 6.3 mg (68%) of dark gray **5**. Spectral data for **5**: IR ν_{CO} (cm^{-1} in CH_2Cl_2): 2087 (m), 2052 (s), 2015 (s), 1971 (w, sh), 1821 (w, br). ^{1}H NMR (in toluene-d_8): $\delta = 1.22$ (d, 27H, CH_3, $^3J_{P-H} = 13$ Hz), -13.86 (d, 2H, hydride, $^1J_{Pt-H} = 774$ Hz, $^2J_{P-H} = 8$ Hz). ^{31}P{^{1}H} NMR (in toluene-d_8): $\delta = 85.3$ (s, 1P, $^1J_{Pt-P} = 4739$ Hz). Anal. Calcd: C, 24.77; H, 2.22. Found: C, 25.13; H, 2.50%.

Synthesis of $Pt_2Ru_5(CO)_{14}(PBu^t_3)_2(\mu\text{-}H)_2(\mu_6\text{-}C)$, 6. A 12.5 mg amount of **5** (0.0096 mmol) was dissolved in 15 mL CH_2Cl_2 in a 50 mL three-neck flask. $Pt(PBu^t_3)_2$ (11.5 mg, 0.019 mmol) was added to the solution, which was then heated to reflux for 1 h. After cooling, the solvent was removed in vacuo and the product was separated by TLC by using a 6:1 hexane/methylene chloride solvent mixture to yield 9.5 mg (58%) of gray **6**. Spectral data for **6**: IR ν_{CO} (cm^{-1} in CH_2Cl_2): 2065 (s), 2040 (s), 2028 (vs), 2001 (s), 1973 (w, sh), 1844 (vw, br), 1817 (w, br). ^{1}H NMR at room temperature (in $CDCl_3$): $\delta = 1.46$ (d, 27H, CH_3, $^3J_{P-H} = 13$ Hz), -14.55 (s, 2H, $^1J_{Pt-H} = 772$ Hz, $^2J_{P-H} = 7$ Hz); ^{1}H NMR at -90 °C (in CD_2Cl_2): $\delta = -13.88$ (dd, H, hydride, $^1J_{Pt-H} = 799$ Hz, $^2J_{P-H} = 15$ Hz, $^3J_{P-H} = 15$ Hz), -15.09 (s, H, hydride, $^1J_{Pt-H} = 706$ Hz). ^{31}P{^{1}H} NMR (in $CDCl_3$): $\delta = 115.4$ (s, 1P, $^1J_{Pt-P} = 6080$ Hz), 83.2 (s, 1P, $^1J_{Pt-P} = 4582$ Hz). Anal. Calcd: C, 29.01; H, 3.71. Found: C, 29.52; H, 2.99%.

Synthesis of $PtRu_5(CO)_{13}(PBu^t_3)](\mu\text{-}H)_3(GePh_3)(\mu_5\text{-}C)$, 7, and $PtRu_5(CO)_{13}(PBu^t_3)(\mu\text{-}H)_2(\mu\text{-}GePh_2)(\mu_6\text{-}C)$, 8. A 16.0 mg amount of **5** (0.012 mmol) was dissolved in 20 mL of heptane in a 50 mL three-neck flask. A 7.5 mg amount of $HGePh_3$ (0.025 mmol) was added, and the solution was heated to reflux for 30 min. The solvent was removed in vacuo, and the products were isolated by TLC by using a 6:1 hexane/methylene chloride solvent mixture to yield, in order of elution, 2.7 mg (15%) of green **8** and 5.6 mg (29%) of dark green **7**. Spectral data for **7**: IR ν_{CO} (cm^{-1} in CH_2Cl_2): 2094 (vs), 2066 (vs), 2039 (vs), 2026 (vs), 1999 (s), 1962 (w). ^{1}H NMR (in $CDCl_3$): $\delta = 1.62$ (d, 27H, CH_3, $^3J_{P-H} = 13$ Hz), -7.47 (s, H, $^1J_{Pt-H} = 558$ Hz, $^2J_{P-H} = 11$ Hz), -21.13 (s, H), -21.48 (s, H). ^{31}P{^{1}H} NMR (in $CDCl_3$): $\delta = 117.8$ (s, 1P, $^1J_{Pt-P} = 2582$ Hz). Anal. Calcd for **7**·$^1/_2(C_6H_{14})$: C, 34.64; H, 3.19. Found: C, 35.06; H, 2.90%. Spectral data for **8**: IR ν_{CO} (cm^{-1} in CH_2Cl_2): 2077 (w), 2047 (vs), 2011 (m), 1990 (w), 1961 (vw). ^{1}H NMR (in $CDCl_3$): $\delta = 1.57$ (d, 27H, CH_3, $^3J_{P-H} = 13$ Hz), -12.28 (dd, H, $^1J_{Pt-H} = 804$ Hz, $^2J_{P-H} = 9$ Hz, $^2J_{H-H} = 9$ Hz), -14.83 (dd, H, $^1J_{Pt-H} = 715$ Hz, $^2J_{P-H} = 5$ Hz, $^2J_{H-H} = 9$ Hz). ^{31}P{^{1}H} NMR (in $CDCl_3$) = 82.5 (s, 1P, $^1J_{Pt-P} = 4773$ Hz). Anal. Calcd: C, 30.26; H, 2.59. Found: C, 30.23; H, 2.43%.

Synthesis of 8 in a Higher Yield. A 15.4 mg amount of **5** (0.012 mmol) was dissolved in 20 mL of heptane in a 50 mL three-neck flask. A 7.0 mg amount of $HGePh_3$ (0.023 mmol) was added, and the solution was heated to reflux for 90 min. The solvent was removed in vacuo and the products were isolated by TLC by using a 6:1 hexane/methylene chloride solvent mixture to yield, in order of elution, 3.8 mg (21%) of **8** and 3.7 mg (20%) of **7**.

Conversion of 7 into 8. A 12.3 mg amount of **7** (0.0078 mmol) was dissolved in 15 mL of heptane in a 50 mL three-neck flask. The solution was heated to reflux for 110 min, and the solvent was then removed in vacuo. The products were separated by TLC by using a 6:1 hexane/methylene chloride solvent mixture to yield 5.3 mg (45%) of **8**.

Synthesis of $PtRu_5(CO)_{13}(PBu^t_3)(\mu\text{-}H)_3(SnPh_3)(\mu_5\text{-}C)$, 9, and $PtRu_5(CO)_{13}(PBu^t_3)(\mu\text{-}H)_2(\mu\text{-}SnPh_2)(\mu_6\text{-}C)$, 10. A 20.0 mg amount of **5** (0.015 mmol) was dissolved in 20 mL of hexane in a 50 mL three-neck flask. An 8.1 mg amount of $HSnPh_3$ (0.023 mmol) was added, and the solution was heated to reflux for 60 min. The solvent was removed in vacuo, and the products were isolated by TLC by using a 6:1 hexane/methylene chloride solvent mixture to yield, in order of elution, 2.3 mg (10%) of green **10** and 2.0 mg (8%) of green **9**. Spectral data for **9**: IR ν_{CO} (cm^{-1} in CH_2Cl_2): 2094 (vs), 2066 (vs), 2040 (vs), 2026 (vs), 1997 (s), 1960 (w). ^{1}H NMR (in $CDCl_3$): $\delta = 1.61$ (d, 27H, CH_3, $^3J_{P-H} = 13$ Hz), -7.49 (s, H, $^1J_{Pt-H} = 559$ Hz, $^2J_{P-H} = 11$ Hz), -21.31 (s, H), -21.69 (s, H). ^{31}P{^{1}H} NMR (in $CDCl_3$): $\delta = 117.9$ (s, 1P, $^1J_{Pt-P} = 2576$ Hz). Anal. Calcd: C, 32.37; H, 2.76. Found: C, 32.47; H, 2.64%. Spectral data for **10**: IR ν_{CO} (cm^{-1} in CH_2Cl_2): 2074 (w), 2048

(3) Adams, R. D.; Captain, B.; Zhu, L. *J. Am. Chem. Soc.* **2004**, *126*, 3042.

(4) (a) Thomas, J. M.; Johnson, B. F. G.; Raja, R.; Sankar, G.; Midgley, P. A. *Acc. Chem. Res.* **2003**, *36*, 20. (b) Raja, R.; Khimyak, T.; Thomas, J. M.; Hermans, S.; Johnson, B. F. G. *Angew. Chem., Int. Ed.* **2001**, *40*, 4638. (c) Hermans, S.; Raja, R.; Thomas, J. M.; Johnson, B. F. G.; Sankar, G.; Gleeson, D. *Angew. Chem., Int. Ed.* **2001**, *40*, 1211. (d) Shephard, D. S.; Maschmeyer, T.; Johnson, B. F. G.; Thomas, J. M.; Sankar, G.; Ozkaya, D.; Zhou, W.; Oldroyd, R. D.; Bell, R. D. *Angew. Chem., Int. Ed. Engl.* **1997**, *36*, 2242. (e) Shephard, D. S.; Maschmeyer, T.; Sankar, G.; Thomas, J. M.; Ozkaya, D.; Johnson, B. F. G.; Raja, R.; Oldroyd, R. D.; Bell, R. G. *Chem. Eur. J.* **1998**, *4*, 12. (f) Braunstein, P.; Rosé, J. Catalysis and Related Reactions with Compounds Containing Heteronuclear Metal−Metal Bonds. In *Comprehensive Organometallic Chemistry II*; Wilkinson, Stone, and Abel, Eds.; Elsevier: Amsterdam, 1995; Vol. 10, Chapter 7. (g) Braunstein, P.; Rose, J. In *Catalysis by Di- and Polynuclear Metal Cluster Complexes*; Adams, R. D., Cotton, F. A., Eds.; VCH: New York, 1998; Chapter 13, p 443. (h) Raja, R.; Sankar, G.; Hermans, S.; Shephard, D. S.; Bromley, S.; Thomas, J. M.; Johnson, B. F. G. *Chem. Commun.* **1999**, 1571. (i) Alexeev, O. S.; Gates, B. C. *Ind. Eng. Chem. Res.* **2003**, *42*, 1571. (j) Ichikawa, M. *Adv. Catal.* **1992**, *38*, 283.

Table 1. Crystallographic Data for Compounds **5**−**7**

compound	**5**	**6**	**7**
empirical formula	$PtRu_5PO_{14}C_{27}H_{29}\cdot 1/2C_4H_{10}O$	$Pt_2Ru_5P_2O_{14}C_{39}H_{56}\cdot C_4H_{10}O$	$PtRu_5GePO_{13}C_{44}H_{45}\cdot 1/2C_6H_{14}$
fw	1345.97	1780.43	1628.89
cryst syst	orthorhombic	triclinic	monoclinic
		Lattice Parameters	
a (Å)	20.5414(9)	12.9564(6)	10.0021(6)
b (Å)	21.3611(9)	14.6621(7)	15.1699(10)
c (Å)	18.4550(8)	14.7665(7)	36.261(2)
α (deg)	90	77.736(1)	90
β (deg)	90	81.399(1)	91.561(1)
γ (deg)	90	83.690(1)	90
V (Å^3)	8097.8(6)	2701.4(2)	5499.8(6)
space group	*Pccn*	$P\bar{1}$	$P2_1/c$
Z value	8	2	4
ρ_{calc} (g/cm^3)	2.208	2.189	1.967
μ (Mo Kα) (mm^{-1})	5.36	6.64	4.49
temp (K)	296	100	296
$2\Theta_{max}$ (deg)	56.6	56.6	56.8
obs reflns ($I > 2\sigma(I)$)	10 069	11 745	10 686
no. params	474	632	619
GOF[a]	1.067	1.117	1.158
max. shift in cycle	0.01	0.008	0.000
residuals[a] R1; wR2	0.0241; 0.0556	0.0389; 0.0682	0.0508; 0.1031
absorption correction,	SADABS	SADABS	SADABS
max/min	1.000/0.549	1.000/0.681	1.000/0.502
largest peak in final diff. map (e$^-$/Å^3)	0.925	1.493	1.368

[a] $R = \sum_{hkl}(||F_{obs}| - |F_{calc}||)/\sum_{hkl}|F_{obs}|$; $R_w = [\sum_{hkl}w(|F_{obs}| - |F_{calc}|)^2/\sum_{hkl}wF_{obs}^2]^{1/2}$, $w = 1/\sigma^2(F_{obs})$; GOF $= [\sum_{hkl}w(|F_{obs}| - |F_{calc}|)^2/(n_{data} - n_{vari})]^{1/2}$.

(vs), 2035 (m), 2010 (m), 1990 (w), 1959 (vw). ^{1}H NMR (in $CDCl_3$): $\delta = 1.59$ (d, 27H, CH_3, $3J_{P-H} = 13$ Hz), −11.81 (dd, H, $^1J_{Pt-H} = 763$ Hz, $^2J_{P-H} = 9$ Hz, $^2J_{H-H} = 9$ Hz), − 14.09 (dd, H, $^1J_{Pt-H} = 751$ Hz, $^2J_{P-H} = 6$ Hz, $^2J_{H-H} = 9$ Hz). ^{31}P{^{1}H} NMR (in $CDCl_3$) = 83.3 (s, 1P, $^1J_{Pt-p} = 4877$ Hz). Anal. Calcd: C, 29.36; H, 2.51. Found: C, 29.44; H, 2.40%.

Synthesis of 9 in an Improved Yield. A 22.0 mg amount of **5** (0.017 mmol) was dissolved in 20 mL of CH_2Cl_2 in a 50 mL three-neck flask. An excess amount of $HSnPh_3$ was added to the solution, and the reaction continued for 5 h at room temperature. The solvent was removed in vacuo, and the product, **9**, was isolated by TLC by using a 5:1 hexane/methylene chloride mixture to yield 16.8 mg (61%).

Conversion of 9 into 10. A 9.8 mg amount of **9** (0.0080 mmol) was dissolved in 15 mL of heptane in a 50 mL three-neck flask. The solution was heated to reflux for 1 h, and the solvent was then removed in vacuo. The products were separated by TLC by using a 6:1 hexane/methylene chloride solvent mixture to yield 2.2 mg (24%) of **10**.

Crystallographic Analyses. Dark red single crystals of **5** and **6** suitable for diffraction analysis were grown by slow evaporation of solvent from a solution of the pure compound in diethyl ether at −20 °C. Dark red single crystals of **7** suitable for diffraction analysis were grown by slow evaporation of solvent from a methylene chloride/hexane solution at −20 °C. Dark single crystals of **8** and red single crystals of **10** suitable for diffraction analysis were grown by slow evaporation of solvent from a solution in a methylene chloride/hexane solvent mixture at 8 °C. Each data crystal was glued onto the end of thin glass fiber. X-ray intensity data were measured using a Bruker SMART APEX CCD-based diffractometer using Mo Kα radiation ($\lambda = 0.71073$ Å). The raw data frames were integrated with the SAINT+ program by using a narrow-frame integration algorithm.[5] Corrections for Lorentz and polarization effects were also applied by SAINT. An empirical absorption correction based on the multiple measurement of equivalent reflections was applied by using the program SADABS. All structures were solved by a combination of direct methods and difference Fourier syntheses, and refined by full-matrix least-squares on F^2 by using the SHELXTL software package.[6] Crystal data, data collection parameters, and results of the analyses for compounds are listed in Tables 1 and 2.

Compound **5** crystallized in the orthorhombic crystal system. The space group *Pccn* was identified uniquely on the basis of the systematic absences in the data, and the structure was solved and successfully refined in this space group. Compound **5** cocrystallizes with half of 1 equiv of diethyl ether in the asymmetric crystal unit. This molecule was also located and satisfactorily refined in the structural analysis. The hydride ligands were located and refined with an isotropic thermal parameter. Compounds **6** and **10** crystallized in the triclinic crystal system. The space group $P\bar{1}$ was assumed and confirmed by the successful solution and refinement of the structure in both cases. All non-hydrogen atoms were refined with anisotropic displacement parameters. In both compounds, the hydride ligands were located and refined with an isotropic thermal parameter. Hydrogen atoms on the phenyl and *tert*-butyl groups for both compounds were placed in geometrically idealized positions and refined as standard riding atoms. Compound **6** cocrystallized with 1 equiv of diethyl ether from the crystallization solvent in the asymmetric crystal unit. The solvent molecule was refined with isotropic thermal parameters. Compounds **7** and **8** crystallized in the monoclinic crystal system. The space group $P2_1/c$ was identified uniquely for each compound on the basis of the systematic absences observed in the data. All non-hydrogen atoms were refined with anisotropic thermal parameters. Compound **7** cocrystallized with half an equivalent of hexane from the crystallization solvent in the asymmetric crystal unit. The hexane subunit was included in the analysis and was refined with isotropic thermal parameters. Three geometric restraints were used in modeling the hexane molecule,

(5) *SAINT+*, version 6.2a; Bruker Analytical X-ray Systems, Inc.: Madison, WI, 2001.

(6) Sheldrick, G. M. *SHELXTL*, version 6.1; Bruker Analytical X-ray Systems, Inc.: Madison, WI, 1997.

Table 2. Crystallographic Data for Compounds **8** and **10**

compound	**8**	**10**
empirical formula	$PtRu_5GePO_{13}C_{38}H_{39}$	$PtRu_5SnPO_{13}C_{38}H_{39}$
fw	1507.69	1553.79
cryst syst	monoclinic	triclinic
	Lattice Parameters	
a (Å)	12.1956(7)	9.7420(4)
b (Å)	18.2670(10)	13.8504(5)
c (Å)	20.5553(12)	18.2328(7)
α (deg)	90	83.783(1)
β (deg)	106.154(1)	87.630(1)
γ (deg)	90	72.989(1)
V (Å^3)	4398.4(4)	2338.38(16)
space group	$P2_1/c$	$P\bar{1}$
Z value	4	2
ρ_{calc} (g/cm^3)	2.277	2.207
μ (Mo Kα) (mm^{-1})	5.609	5.166
temp (K)	100	296
$2\Theta_{max}$ (deg)	56.6	56.6
obs reflns ($I > 2\sigma(I)$)	10 088	9465
no. params	549	548
GOF[a]	1.093	0.997
max. shift in cycle	0.006	0.002
residuals[a] R1; wR2	0.0276; 0.0309	0.0279; 0.0598
absorption correction,	SADABS	SADABS
max/min	1.000/0.433	1.000/0.650
largest peak in final diff. map (e$^-$/Å^3)	2.123	0.925

[a] $R = \sum_{hkl}(||F_{obs}| - |F_{calc}||)/\sum_{hkl}|F_{obs}|$; $R_w = [\sum_{hkl}w(|F_{obs}| - |F_{calc}|)^2/\sum_{hkl}wF_{obs}^2]^{1/2}$, $w = 1/\sigma^2(F_{obs})$; GOF $= [\sum_{hkl}w(|F_{obs}| - |F_{calc}|)^2/(n_{data} - n_{vari})]^{1/2}$.

which was disordered about an inversion center. Hydrogen atoms were placed in geometrically idealized positions and included as standard riding atoms.

Results and Discussion

The new dihydrido platinum−ruthenium cluster complex **5** was obtained in 68% yield from the reaction of **3** with hydrogen (1 atm) in a heptane solution at reflux for 1.5 h. Compound **5** was characterized by a combination of IR, ^{1}H NMR, ^{31}P NMR, and single-crystal X-ray diffraction analyses. An ORTEP diagram of the molecular structure of **5** is shown in Figure 1. The molecule consists of a $PtRu_5$ cluster in the shape of an octahedron with an interstitial carbido ligand C(1) in the center. A PBu^t_3 ligand is coordinated to the platinum atom and one CO ligand, C(53)−O(53), bridges the Ru(4)−Ru(5) bond. There are also two hydrido ligands (located and refined crystallographically) that bridge two of the Pt−Ru bonds. The Pt−H bond distances appear to be significantly shorter than the Ru−H distances, Pt(1)−H(1) = 1.67(4) Å, Pt(1)−H(2) = 1.71(4) Å, Ru(2)−H(1) = 1.90(4) Å, and Ru(4)−H(2) = 1.89(4) Å, although the errors are relatively large. In contrast to most examples, these hydride-bridged metal−metal bonds, Pt(1)−Ru(4) = 2.8336(3) Å, Pt(1)−Ru(2) = 2.8497(3) Å, are significantly shorter than the unbridged Pt−Ru bonds, Pt(1)−Ru(3) = 2.9969(3) Å, Pt(1)−Ru(1) = 3.1189(3) Å.[7] It has been shown that in the presence of additional bridging ligands, such as an interstitial carbido ligand, the lengthening effects of bridging hydride ligands on metal−metal bonds are often not observed.[7] One possible reason the unbridged Pt−Ru bonds in

(7) Teller, R. G.; Bau, R. *Struct. Bonding* **1981**, *41*, 1.

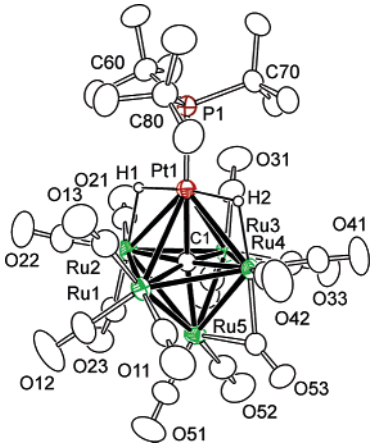

Figure 1. An ORTEP diagram of $PtRu_5(CO)_{14}(PBu^t_3)(\mu\text{-}H)_2(\mu_6\text{-}C)$, **5**, showing 40% probability thermal ellipsoids. Selected interatomic distances (Å) are Pt(1)−Ru(4) = 2.8336(3), Pt(1)−Ru(2) = 2.8497(3), Pt(1)−Ru(3) = 2.9969(3), Pt(1)−Ru(1) = 3.1189(3), Pt(1)−H(1) = 1.67(4), Pt(1)−H(2) = 1.71(4), Ru(2)−H(1) = 1.90(4), Ru(4)−H(2) = 1.89(4), Pt(1)−P(1) = 2.3248(9), Ru(1)−Ru(5) = 2.7703(4), Ru(1)−Ru(2) = 2.8840(4), Ru(1)−Ru(4) = 2.9691(4), Ru(2)−Ru(3) = 2.8571(4), Ru(2)−Ru(5) = 3.1030(4), Ru(3)−Ru(5) = 2.7896(4), Ru(3)−Ru(4) = 2.9708(4), Ru(4)−Ru(5) = 2.8378(4).

5 are actually longer than the hydride-bridged Pt−Ru bonds could be due to steric interactions between the CO ligands on the ruthenium atoms and the PBu^t_3 ligand on the platinum atom. In particular, ruthenium atoms Ru(1) and Ru(3) both have one carbonyl ligand that is projected toward the methyl groups on the PBu^t_3 ligand. This resultant repulsion effects could cause the associated platinum−ruthenium bond distances to increase slightly, as observed. These effects would not be present for the ruthenium atoms bonded to the bridging hydrido ligands because the CO ligands on these atoms are not projected toward the PBu^t_3 group.

Although they are not equivalent in the structure observed in the solid state, the hydrido ligands are equivalent in the ^{1}H NMR spectrum and show strong one-bond coupling to ^{195}Pt: $\delta = -13.86$ (d,$^1J_{Pt-H} = 774$ Hz, $^2J_{P-H} = 8$ Hz). Interconversion of the environments of the two hydrido ligands could be obtained by a simple motion involving two of the carbonyl ligands, one on Ru(2) and the bridge between Ru(4) and Ru(5). In particular, if the terminal CO ligand, C(23)−O(23), on Ru(2) moved into a bridging position across the Ru(2)−Ru(5) bond and the bridging CO ligand, C(53)−O(53), moved into a terminal position on Ru(4), then the environments of the two hydrido ligands would be interchanged.

When compound **5** was treated with $Pt(PBu^t_3)_2$, the new complex $Pt_2Ru_5(CO)_{14}(PBu^t_3)_2(\mu\text{-}H)_2(\mu_6\text{-}C)$, **6**, was formed in 58% yield. Compound **6** was characterized by a combination of IR, ^{1}H NMR, ^{31}P NMR, and single-crystal X-ray diffraction analyses, and an ORTEP diagram of its molecular structure is shown in Figure 2. Compound **6** can be viewed as a $Pt(PBu^t_3)$ adduct of **5** formed by adding a $Pt(PBu^t_3)$ grouping across one of the Ru−Ru bonds in the base of the square pyramidal part of the Ru_5 portion of the cluster of **5**, specifically either the Ru(1)−Ru(2) bond or Ru(2)−Ru(4) bond. The added $Pt(PBu^t_3)$ group is structurally similar to the bridging $Pt(PBu^t_3)$ group found on the edge of **3b** in the

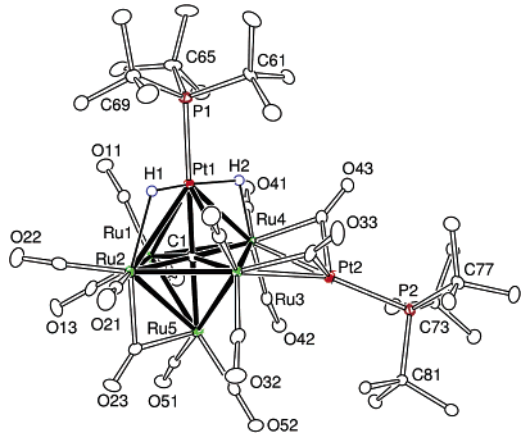

Figure 2. An ORTEP diagram of $Pt_2Ru_5(CO)_{14}(PBu^t_3)_2(\mu\text{-}H)_2(\mu_6\text{-}C)$, **6**, showing 40% probability thermal ellipsoids. Selected interatomic distances (Å) are Pt(1)−P(1) = 2.3344(14), Pt(1)−Ru(1) = 3.1407(5), Pt(1)−Ru(2) = 2.8835(5), Pt(1)−Ru(3) = 2.8972(5), Pt(1)−Ru(4) = 2.8561(5), Pt(2)−P(2) = 2.3416(14), Pt(2)−Ru(3) = 2.8146(5), Pt(2)−Ru(4) = 2.7618(5), Ru(1)−Ru(5) = 2.7654(6), Ru(1)−Ru(4) = 2.8820(6), Ru(1)−Ru(2) = 2.9364(6), Ru(2)−Ru(3) = 2.8492(6), Ru(2)−Ru(5) = 2.8704(6), Ru(3)−Ru(4) = 3.0073(6), Ru(3)−Ru(5) = 2.8719(6), Ru(4)−Ru(5) = 2.9881-(6), Pt(1)−H(1) = 1.3(1), Pt(1)−H(2) = 1.65(7), Ru(2)−H(1) = 2.23(10), Ru(4)−H(2) = 1.88(6).

open structure of **3**. One carbonyl ligand bridges each of the Pt−Ru bonds to the added $Pt(PBu^t_3)$ group, as found in **3b**, and also in the two alkyne complexes $Pt_2Ru_5(CO)_{13}$-$(PBu^t_3)_2(\mu_5\text{-}C)(\mu_3\text{-}PhC_2H)$, **11**, and $Pt_3Ru_5(CO)_{13}(PBu^t_3)_3$-$(\mu_5\text{-}C)(\mu_3\text{-}PhC_2H)$, **12**.[8]

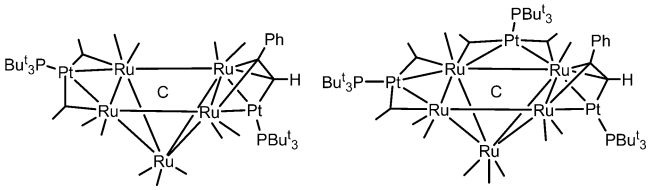

11 **12**

The two hydrido ligands in **6** were located in the structural analysis. They bridge the Pt(1)−Ru(2) and Pt(1)−Ru(4) bonds that are the two shortest Pt−Ru bonds, 2.8835(5) and 2.7618(5) Å, respectively, but the Pt(1)−Ru(3) = 2.8972-(5) Å is nearly as short as the Pt(1)−Ru(2) bond. The Pt(1)−Ru(1) bond is very long, 3.1407(5) Å. As in **5**, these metal−metal bond distances seem to be related to steric interactions between CO ligands and the PBu^t_3 ligand on the neighboring Pt atom. The hydrido ligands in **6** are inequivalent. In accord with this, two highly shielded resonances were observed in the ^{1}H NMR spectrum of **6** at −90 °C, −13.6 and −15.1 ppm. Interestingly, however, these resonances broadened and merged into a singlet that was sharp at −14.55 ppm (with appropriate ^{195}Pt−H coupling) at room temperature, see Figure 3. These changes are indicative of a dynamical exchange process that rapidly averages the environments of the two hydrido ligands on the NMR time scale at room temperature. The rate of exchange at the coalescence temperature (k_c) was estimated by using the expression $k_c = \pi\Delta\nu_0/(2)^{1/2}$, where $\Delta\nu_0$ is the chemical shift difference between the resonances in the slow exchange limit. Substitution of the k_c rate into the Eyring equation provided the free energy of activation for the process at the coalescence temperature, $\Delta G^\dagger$ (at 228 K) = 10.0(5) kcal/mol. Facile dynamical activity in compounds **3** and **12** which involves motion of their edge-bridging $Pd(PBu^t_3)$ and $Pt(PBu^t_3)$ groups has been described previously.[1b,2,8]

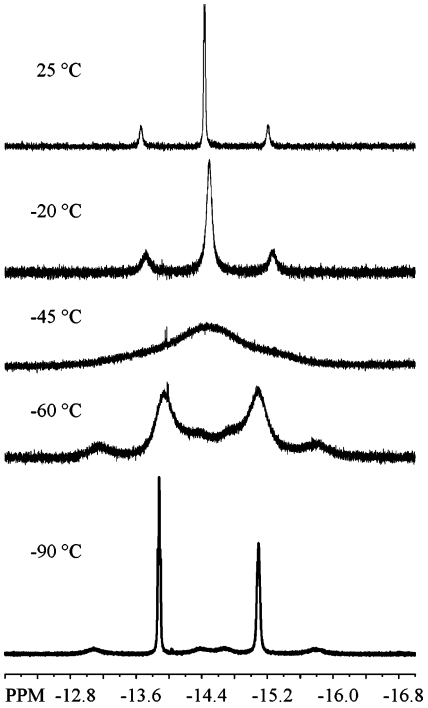

Figure 3. Variable-temperature ^{1}H NMR spectra for compound **6** in CD_2Cl_2 solvent.

For the sake of completeness, three mechanisms for the averaging of the hydrido ligands in **6** have been considered, and these are shown in Scheme 1. The possible mechanisms are divided into two categories: (A) shifts involving the edge-bridging $Pt(PBu^t_3)$ group and (B) shifts involving the hydrido ligands. By process (A) the $Pt(PBu^t_3)$ group is shifted from the Ru−Ru bond, Ru(3)−Ru(4), that is proximate to the hydrido ligand H(2) to the Ru−Ru bond, Ru(2)−Ru(3), that is proximate to the second hydrido ligand H(1). This would interchange the environments of hydrido ligands, i.e., **6** goes to its equivalent from **6′** and vice versa. Two mechanisms for the type (A) process have been considered: (1) intramolecular shifts and (2) a dissociation and reassociation of the $Pt(PBu^t_3)$ group. The dissociative mechanism must be considered seriously because of the absence of observable long-range couplings between the hydrido ligands and the Pt or P atoms of the appended $Pt(PBu^t_3)$ group in the fast-exchange region of the spectra. In general, these couplings would be observed in a nondissociative process; however, if the $Pt(PBu^t_3)$ group is dissociated from the cluster during the exchange process, these couplings would be lost. Note, however, that these couplings were also not observed in the spectra of **6** in the slow-exchange region, so one might not necessarily expect to them to appear in the fast-exchange region. If the $Pt(PBu^t_3)$ group dissociates fully from **6**, then the compound **5** and an isolated $Pt(PBu^t_3)$ fragment would be formed as an intermediate, see process (2) in Scheme 1.

(8) Adams, R. D.; Captain, B.; Zhu, L. *Organometallics* **2005**, *24*, 2419.

Scheme 1

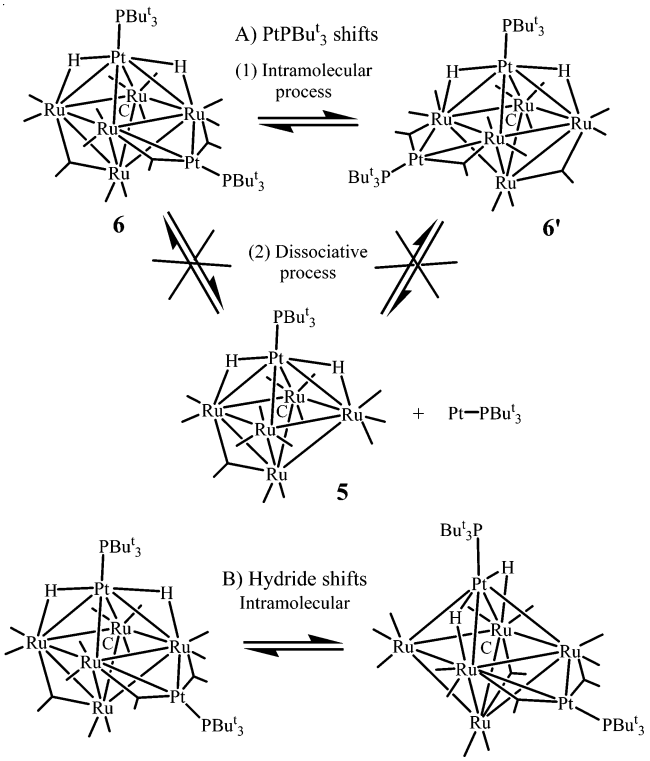

The following test for the Pt(PBu$^t_3$) dissociative process (2) was performed. An equimolar quantity of **5** was added to a sample of **6**, and the ^{1}H NMR spectrum of the mixture was recorded at room temperature (i.e., the fast-exchange region of **6**). If molecule **6** is dissociating its Pt(PBu$^t_3$) group to generate **5**, then the released Pt(PBu$^t_3$) group could return either to the molecule of **5** that was generated, or any other molecule of **5** that might be present in the sample. So if a truly dissociative process were operative, then the signals of **6** and the added **5** in the mixed sample would be averaged. However, in the mixed sample, separate and sharp resonances both for the added **5** and for the dynamically active **6** were observed. The conclusion is that the Pt(PBu$^t_3$) group is probably not dissociating. This leaves the two intramolecular mechanisms: A (1) shifts of the Pt(PBu$^t_3$) group or B intramolecular shifts the hydrido ligands with a static Pt(PBu$^t_3$) group.[9,10] On the basis of observations of the static hydrido ligands in the ^{1}H NMR spectra of the compounds **8** and **10** at room temperature, vide infra, a mechanism involving shifts of the Pt(PBu$^t_3$) group is favored,[1b,2,8] but the hydride shift mechanism cannot be completely ruled out for this system. Compound **6** contains a total of 98 valence electrons. This is two less than the number, 100, expected for an edge-bridged octahedron, 86 + 14.[11] The reason for this is because the edge-bridging platinum atom in **6** has only a 16 electron configuration instead of the usual 18 electron configuration of a typical transition metal atom.

(9) A process involving dissociation of hydrogen atoms or hydrogen ions in these nonpolar solvents seems highly unlikely.
(10) A shift in the location of the bridging CO ligand is required by all mechanisms.
(11) Mingos, D. M. P. *Acc. Chem. Res.* **1984**, *17*, 311.

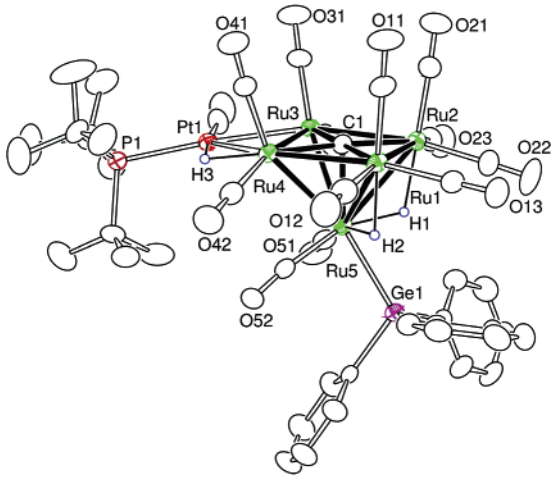

Figure 4. An ORTEP diagram of PtRu$_5$(CO)$_{13}$(PBu$^t_3$)](μ-H)$_3$(GePh$_3$)-(μ_5-C), **7**, showing 30% probability thermal ellipsoids. Selected interatomic distances (Å) are Pt(1)−P(1) = 2.3745(18), Pt(1)−H(3) = 1.79(7), Pt(1)−Ru(3) = 2.6683(6), Pt(1)−Ru(4) = 2.8363(6), Ru(1)−Ru(2) = 2.8654(8), Ru(1)−Ru(4) = 2.8627(8), Ru(1)−Ru(5) = 2.8831(7), Ru(1)−H(2) = 1.85-(8), Ru(2)−Ru(3) = 2.8892(7), Ru(2)−Ru(5) = 2.8821(7), Ru(2)−H(1) = 1.86(5), Ru(3)−Ru(4) = 2.7414(7), Ru(3)−Ru(5) = 2.9392(7), Ru(4)−Ru(5) = 2.8742(7), Ru(4)−H(2) = 1.70(8), Ru(5)−H(1) = 1.66(5), Ru(5)−H(2) = 1.85(8), Ru(5)−Ge(1) = 2.5362(8).

In recent studies, we have shown that HGePh$_3$[12] and HSnPh$_3$[13] can be readily added to ruthenium, rhodium, iridium, and rhenium carbonyl cluster complexes to yield products containing phenylgermyl and phenylstannyl groups, respectively. For purposes of comparison, we have also investigated the reactions of **5** with HGePh$_3$ and HSnPh$_3$.

Two new bimetallic cluster complexes, **7** and **8**, were obtained in 29% and 15% yield, respectively, when a solution of **5** and HGePh$_3$ in heptane solvent was heated to reflux for 30 min. Compound **8** can be converted directly from **7** in 45% yield by heating to reflux in a heptane solution for 110 min. Both new products were characterized by a combination of IR, ^{1}H NMR, ^{31}P NMR, and single-crystal X-ray diffraction analyses. An ORTEP diagram of the molecular structure of **7** is shown in Figure 4. The structure of **7** contains an open PtRu$_5$ cluster similar to that of **3b** with the Pt(PBu$^t_3$) group bridging one edge of the base of the Ru$_5$ square pyramid. A Ph$_3$Ge ligand is coordinated to the apical ruthenium atom Ru(5), Ru(5)−Ge(1) = 2.5362-(8) Å. Compound **7** contains three hydride ligands. All three were located and refined in the structural analysis. H(1) and H(2) bridge the two of the apical−basal Ru−Ru edges, Ru(1)−Ru(5) and Ru(2)−Ru(5), of the Ru$_5$ square pyramid cis to the Ph$_3$Ge ligand. The third hydride ligand H(3) bridges the Pt(1)−Ru(4) bond. Notably, the hydride-bridged Pt(1)−Ru(4) bond distance, 2.8363(6) Å, is much longer than the unbridged Pt(1)−Ru(3) bond of 2.6683(6) Å, presumably due in part to the presence of this bridging hydride ligand.

(12) (a) Adams, R. D.; Captain, B.; Fu, W. *Inorg. Chem.* **2003**, *42*, 1328. (b) Adams, R. D.; Captain, B.; Smith, J. L., Jr. *Inorg. Chem.* **2005**, *44*, 1413.
(13) (a) Adams, R. D.; Captain, B.; Fu, W.; Smith, M. D. *Inorg. Chem.* **2002**, *41*, 5593. (b) Adams, R. D.; Captain, B.; Smith, J. L., Jr.; Hall, M. B.; Beddie, C. L.; Webster, C. E. *Inorg. Chem.* **2004**, *43*, 7576. (c) Adams, R. D.; Captain, B.; Johansson, M.; Smith, J. L., Jr. *J. Am. Chem. Soc.* **2005**, *127*, 489.

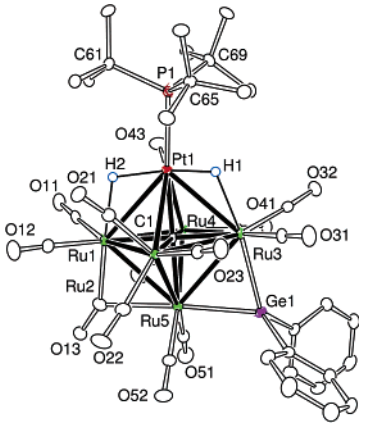

Figure 5. An ORTEP diagram of $PtRu_5(CO)_{13}(PBu^t_3)(\mu\text{-}H)_2(\mu\text{-}GePh_2)(\mu_6\text{-}C)$, **8**, showing 40% probability thermal ellipsoids. Selected interatomic distances (Å) are Pt(1)−P(1) = 2.3294(8), Pt(1)−H(1) = 1.44(6), Pt(1)−H(2) = 1.63(6), Pt(1)−Ru(1) = 2.9006(3), Pt(1)−Ru(2) = 2.9159(3), Pt(1)−Ru(3) = 2.8501(3), Pt(1)−Ru(4) = 3.0459(3), Ru(1)−H(2) = 1.97(5), Ru(1)−Ru(2) = 2.8274(4), Ru(1)−Ru(4) = 2.8635(4), Ru(1)−Ru(5) = 2.9169(4), Ru(2)−Ru(3) = 3.0059(4), Ru(2)−Ru(5) = 2.8772(4), Ru(3)−Ge(1) = 2.4696(4), Ru(3)−H(1) = 2.00(5), Ru(3)−Ru(4) = 2.9619(4), Ru(3)−Ru(5) = 2.9325(4), Ru(4)−Ru(5) = 2.8141(4), Ru(5)−Ge(1) = 2.4788(4).

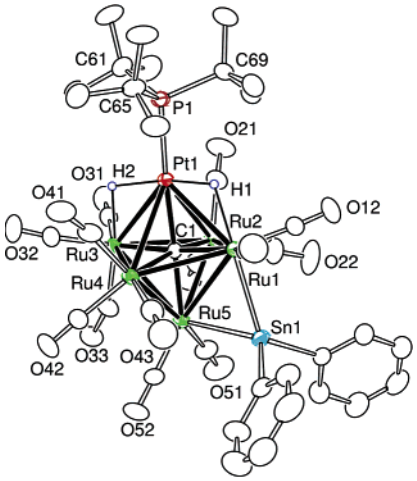

Figure 6. An ORTEP diagram of $PtRu_5(CO)_{13}(PBu^t_3)(\mu\text{-}H)_2(\mu\text{-}SnPh_2)(\mu_6\text{-}C)$, **10**, showing 30% probability thermal ellipsoids. Selected interatomic distances (Å) are Pt(1)−P(1) = 2.3255(10), Pt(1)−H(1) = 1.68(5), Pt(1)−H(2) = 1.73(5), Pt(1)−Ru(1) = 2.8171(3), Pt(1)−Ru(2) = 3.0621(3), Pt(1)−Ru(3) = 2.8483(3), Pt(1)−Ru(4) = 3.0650(3), Ru(1)−H(1) = 1.92(5), Ru(1)−Sn(1) = 2.6209(4), Ru(5)−Sn(1) = 2.6469(4), Ru(1)−Ru(2) = 2.9612(4), Ru(1)−Ru(4) = 2.9787(4), Ru(1)−Ru(5) = 3.0023(4), Ru(2)−Ru(3) = 2.8756(4), Ru(2)−Ru(5) = 2.7926(4), Ru(3)−H(2) = 1.88(5), Ru(3)−Ru(4) = 2.8655(4), Ru(3)−Ru(5) = 2.9802(4), Ru(4)−Ru(5) = 2.7881(4).

The resonance of hydride H(3) was observed at −7.47 ppm and shows the expected coupling to ^{195}Pt and ^{31}P, ($^1J_{Pt-H}$ = 558 Hz, $^2J_{P-H}$ = 11 Hz) in the ^{1}H NMR spectrum of **7**. The more highly shielded resonances of H(1) and H(2) were observed at −21.13 and −21.48 ppm, respectively, and have no observable couplings to the platinum or phosphorus atoms. Compound **7** contains 86 valence electrons. This is two less than the number, 88, expected for an edge-bridged square pyramid, 74 + 14.[11] The reason for this is because in **7** the edge-bridging platinum atom has only a 16 electron configuration instead of the usual 18 electron configuration of a typical transition metal atom.

An ORTEP diagram of the molecular structure of **8** is shown in Figure 5. The structure of the cluster of **8** is very similar to that of **5** and contains a closed $PtRu_5$ cluster where the $Pt(PBu^t_3)$ group bridges the entire base of the Ru_5 square pyramid. Compound **8** contains only two hydrido ligands, H(1) and H(2), that bridge oppositely positioned Pt−Ru bonds, Pt(1)−H(1) = 1.44(6) Å, Pt(1)−H(2) = 1.63(6) Å, Ru(1)−H(2) = 1.97(5) Å, and Ru(3)−H(1) = 2.00(5) Å. As in **5**, the hydride-bridged metal−metal bonds, Pt(1)−Ru(1) = 2.9006(3) Å and Pt(1)−Ru(3) = 2.8501(3) Å, are shorter than the unbridged bonds, Pt(1)−Ru(2) = 2.9159(3) Å and Pt(1)−Ru(4) = 3.0459(3) Å. The hydride ligands are inequivalent, and accordingly, two resonances were observed for them in the ^{1}H NMR spectrum, δ = −12.28 (dd, H, $^1J_{Pt-H}$ = 804 Hz,$^2J_{P-H}$ = 9 Hz, $^2J_{H-H}$ = 9 Hz) and −14.83 (dd, H, $^1J_{Pt-H}$ = 715 Hz,$^2J_{P-H}$ = 5 Hz, $^2J_{H-H}$ = 9 Hz). It is noteworthy that, unlike **5**, there was no evidence for dynamical exchange between these hydride ligands on the NMR time scale at room temperature. Compound **8** also contains a $GePh_2$ ligand that bridges the Ru(3)−Ru(5) bond. The Ru−Ge bond distances, Ru(3)−Ge(1) = 2.4696(4) Å and Ru(5)−Ge(1) = 2.4788(4) Å, are similar to those found in the related compounds $Ru_5(CO)_{12}(\mu_5\text{-}C)(\mu\text{-}H)_2(\mu\text{-}GePh_2)_4$ and $Ru_5(CO)_{11}(\mu_5\text{-}C)(\mu\text{-}H)_2(\mu\text{-}GePh_2)_4$, which range from 2.47 to 2.50 Å.[12a] Compound **8** has structural similarities to the compound $PtRu_5(CO)_{15}(\mu_6\text{-}C)(\mu\text{-}GePh_2)$, **13**, that was

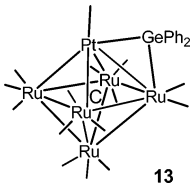

13

obtained from the reaction of $PtRu_5(CO)_{16}(\mu_6\text{-}C)$ with $HGePh_3$, but compound **13** has no hydrido ligands and the $GePh_2$ ligand in **13** bridges one of the Pt−Ru bonds, Pt−Ge = 2.4701(6) Å and Ru−Ge = 2.4457(8) Å.[14] Compound **8** contains 86 valence electrons. This is precisely the number expected for a closo-octahedron.[13]

The bimetallic cluster complexes **9** and **10** were obtained in low yields, 8% and 10% yield, respectively, from the reaction of **5** with $HSnPh_3$ in a hexane solution at reflux for 30 min. Compound **9** was obtained in a much better yield (61%) when the reaction was performed at room temperature in CH_2Cl_2 solvent over 5 h, but no **10** was formed at this temperature. Compound **10** can be obtained directly from **9** in a 24% yield by heating a solution in heptane solvent at reflux for 1 h. Both new compounds were characterized by a combination of IR, ^{1}H NMR, and ^{31}P NMR analysis. Attempts to obtain a high quality single-crystal X-ray diffraction analysis of **9** were unsuccessful due to crystallographic disorder problems, but the partial analysis clearly showed a structure similar to that of **7**. This is supported by the strong similarities between the IR and NMR spectra of

(14) Adams, R. D.; Captain, B.; Fu, W. *J. Organomet. Chem.* **2003**, *671*, 158.

Scheme 2

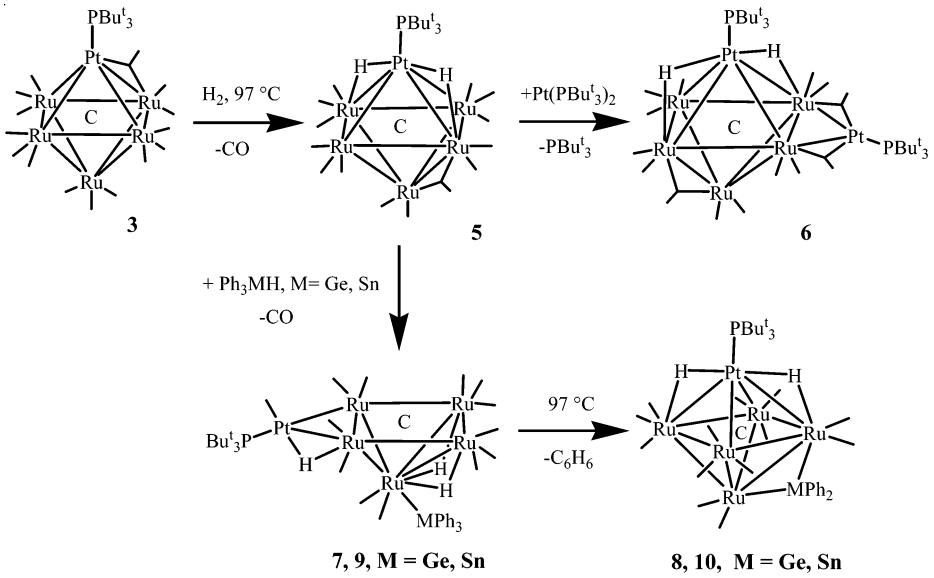

7 and **9**. Compound **9** contains three hydride ligands, and the ^{1}H NMR spectrum shows that one of these ligands is proximate to the platinum atom as in **7**, $\delta = -7.49$, $^1J_{Pt-H} = 559$ Hz, and two are remote to platinum, $\delta = -21.31$ and -21.69 with no observable couplings to the platinum or phosphorus atoms.

Compound **10** was successfully characterized by a single-crystal X-ray diffraction analyses, and an ORTEP diagram of its molecular structure is shown in Figure 6. The structure of **10** is virtually the same as that of **8** except that it contains an $SnPh_2$ ligand bridging the Ru−Ru bond in place of the $GePh_2$ ligand. The Ru−Sn bond distances, Ru(1)−Sn(1) = 2.6209(4) Å and Ru(5)−Sn(1) = 2.6469(4) Å, are considerably longer than the Ru−Ge bonds in **8**, but are very similar to the Ru−Sn bond distances that range from 2.60 to 2.73 Å to the bridging $SnPh_2$ ligands found in the related compounds $Ru_5(CO)_{10}(SnPh_3)(\mu\text{-}SnPh_2)_4(\mu_5\text{-}C)(\mu\text{-}H)$, $Ru_5(CO)_8(\mu\text{-}SnPh_2)_4(C_6H_6)(\mu_5\text{-}C)$, and $Ru_5(CO)_7(\mu\text{-}SnPh_2)_4(SnPh_3)(C_6H_6)(\mu_5\text{-}C)(\mu\text{-}H)$.[12a] The compound $PtRu_5(CO)_{15}(\mu_6\text{-}C)(\mu\text{-}SnPh_2)$, **14**, which is similar to **13**, contains a $SnPh_2$ ligand bridging one of the Pt−Ru bonds, Pt−Sn = 2.5825(6) Å and Ru−Sn = 2.6590(6) Å.[14] Compound **10** also contains two inequivalent hydrido ligands, H(1) and H(2), that bridge oppositely positioned Pt−Ru bonds: Pt(1)−H(1) = 1.68(5) Å, Pt(1)−H(2) = 1.73(5) Å, Ru(1)−H(1) = 1.92(5) Å, and Ru(3)−H(2) = 1.88(5) Å. These inequivalent hydrido ligands exhibit separate resonances at room temperature in the ^{1}H NMR spectrum, $\delta = -11.81$ (dd, H, $^1J_{Pt-H} = 763$ Hz, $^2J_{P-H} = 9$ Hz, $^2J_{H-H} = 9$ Hz) and -14.09 (dd, H, $^1J_{Pt-H} = 751$ Hz, $^2J_{P-H} = 6$ Hz, $^2J_{H-H} = 9$ Hz), and as with **8**, there is no evidence for dynamical exchange between them on the NMR time scale at room temperature.

A summary of the reactions investigated in this study is shown in Scheme 2. The reaction of **3** with hydrogen proceeds by the loss of one CO ligand from **3** and the oxidative addition of 1 equiv of H_2 to the cluster to form compound **5**. The valence electron count for **5** is the same as that for **3**, 86 electrons, which is in accord with the standard electron-counting theories.[11] Compound **5** forms a $Pt(PBu^t_3)$ adduct **6** by adding a $Pt(PBu^t_3)$ group across one of the Ru−Ru bonds in the square base of the Ru_5 portion of the cluster of **5**. Compound **6** is dynamically active on the NMR time scale by a mechanism that appears to involve a shifting of the $Pt(PBu^t_3)$ group from one Ru−Ru bond to another instead of a hydride-shift mechanism. This conclusion is based on the considerable precedence for $Pt(PBu^t_3)$ dynamical shift processes observed in related molecules, such as **3** and **12**, and the absence of a dynamical hydride shift process in the closely related compounds **8** and **10**. Compound **5** reacts with $HGePh_3$ and $HSnPh_3$ by loss of CO and the oxidative addition of the M−H bond, M = Ge or Sn, to the cluster to yield the products **7** and **9**, respectively. The MPh_3 group is coordinated to the apical ruthenium atom of the Ru_5 square pyramid in the products, which is probably the site of the M−H oxidative addition. The apical Ru site is probably the least sterically encumbered in the molecule, and this is probably why the oxidative addition occurs there. However, replacing a CO ligand on the apical ruthenium atom with a bulky MPh_3 group is certain to increase the ligand sterics throughout the entire molecule in the products, and this would be one reason the cluster has opened to form a Pt-bridged square pyramidal Ru_5 cluster. This opening of the cluster is a notable contrast to the oxidative addition of H_2 to **3** to give **5** which contains a closed M_6 cluster. When heated, compounds **7** and **9** both lose benzene to form **8** and **10**, respectively. The formation of benzene was confirmed by ^{1}H NMR spectroscopy. The MPh_2 ligand that is formed occupies a bridging position across one of the neighboring apical−basal Ru−Ru bonds of the Ru_5 square pyramid. The MPh_2 ligands are sterically smaller than the MPh_3 ligands, and as a result, the metal cluster then closes to the octahedral structure.

Acknowledgment. This research was supported by the Office of Basic Energy Sciences of the U.S. Department of

Energy under Grant No. DE-FG02-00ER14980. We thank STREM for donation of a sample of $Pt(PBu^t_3)_2$ and Dr. Perry J. Pellechia for his valuable assistance with the variable temperature NMR measurements.

Supporting Information Available: X-ray and CIF tables for the structural analyses of compounds **5**−**8** and **10**. This material is available free of charge via the Internet at http://pubs.acs.org.

IC051007Q